2010-019731）。

以上の結果は、多価型ペプチドライブラリー法と多価型ペプチドシートスクリーニング法を組み合わせることにより、取得できるモチーフ種を飛躍的に増やすことができることを示している。さらに、今回サブトラクションに使用した変異体はG62Aであるにもかかわらず G62特異的な結合モチーフが取得できることから、わずかメチル基１つ分の相違を識別する分解能を持ったモチーフが取得可能であることを示している。

その一方で、本シートを用いて、Stx1a 以外の全てのバリアントに対する結合活性を同様に調べ、各々の結合特異性を比較検討しようとする場合、数十枚のレベルでシートのコピーが必要となる。しかしながら、このレベルでのコピー作製は、現技術ではコストならびに時間的制約のため極めて困難である。そこで本問題の解決を目指し、スライドグラスを基盤とした多価型ペプチドのスポット合成技術の確立を試みた。

C.2.　スライドグラスを基盤とした多価型ペプチドライブラリー作製技術の確立

多価型ペプチドライブラリー法と Intavis 社のスライドスポッターを組み合わせ、1 枚のスライドグラス上に最大 768 種類の多価ペプチドをスペーサーを介してスポット状に合成する新たな系を確立する。このとき、スペーサーを介して結合した多価ペプチドの基盤上の密度、ならびに基盤面からの距離を標的タンパク質に対して立体的に最適化する（添付図２）。本スライドスポッターの最大の特徴は、一度に 29 枚のコピー作製が可能な点である。従って、先のセルロースシートを用いた際の問題点を解決することができると期待される。

本系では、シート合成用のセルロースに比較してアミノ基の密度が 2.5 倍高いディスク状のセルロースを用い、１つのディスク上に多価型ペプチドを１種類ずつ合成してから溶解し、スライドスポッターを用いてスライドグラス上へと固定してゆく。このため、スペーサー長ならびに種類、結合させる多価ペプチドの基盤上の密度、などの合成条件、さらにブロット後標的タンパクを高感度に検出するための条件，等を新たに最適化する必要がある。このため、すでに取得している Stx1a B-subunit のサイト１を標的として取得した阻害モチーフを用いた検討が進行中である。

D. 結論

多価型ペプチドライブラリー法と多価型ペプチドシートスクリーニング法を組み合わせることにより、標的分子に対する高親和性結合モチーフの取得効率を飛躍的に亢進させる系が確立できた。さらにモチーフ取得の効率ならびに精度を一層促進させるため、スライドグラスを基盤とした多価型ペプチドライブラリー作製技術の確立を目指している。上記手法ではモチーフ決定にアミノ酸シークエンスを用いないため、ユニットとしての構成分子にアミノ酸を使用するという制約がない。このため、様々なアミノ酸誘導体、低分子化合物がユニットとして使用可能である。さらに、デンドリマー化や PEG 化などにより、分子全体としての形状多様化も可能である。これらの新規ユニットを用いることにより、格段に高精度化した高親和性化合物の取得が可能になると期待される。

系が確立し次第、細菌毒素以外にも細胞内情報伝達を担うシグナル分子群（各種 protein kinase、シグナル伝達分子等）を標的とした制御分子開発へと発展させてゆく。

E. 健康危機情報

なし

F. 研究発表等

1) Kato M., Watanabe-Takahashi M., Shimizu E., and Nishikawa K.: Identification of a wide range of motifs inhibitory to Shiga toxin by affinity-driven screening of customized divalent peptides synthesized on a membrane. *Appl. Environ. Microbiol.*, 2015; 81: 1092-1100.

学会発表等

1) 西川喜代孝:AB5 型細菌毒素に対する多価型ペプチド性阻害薬の開発. 第８８回日本細菌学会総会（2014. 3, 岐阜).
2) 高橋美帆、清水英子、加藤美帆子、西川喜代孝：異なった受容体結合部位を標的とする Stx 阻害薬の併用による相乗効果. 第８８回日本細菌学会総会（2014. 3, 岐阜).
3) 近江 純平、高橋 美帆、宮坂 知宏、山崎 伸二、日高 雄二、杤尾 豪人、濱端 崇、西川喜代孝：耐熱性エンテロトキシンに対するペプチド性阻害薬開発. 第８８回日本細菌学会総会（2014. 3, 岐阜).
4) 雲井香保里、高橋美帆、山本洋、濱端崇、西川喜代孝：新規ペプチド性コレラ毒素阻害薬の in vivo での効果. 第８８回日本細菌学会総会（2014. 3, 岐阜).
5) 小川莉奈、宮崎俊秀、長尾耕治郎、原雄二、佐々木善浩、秋吉一成、稲葉岳彦、小林俊彦、高橋美帆、西川喜代孝、梅田真郷：ホスファチジン酸結合性を有する４価型人工ペプチドの開発. 第８７回日本生化学会大会（2014. 10, 京都).
6) 高橋美帆、清水英子、加藤美帆子、西川喜代孝：受容体結合部位特異的 Stx 阻害薬の組み合わせによる阻害効果の増強. 第１８回腸管出血性大腸菌感染症研究会(2014. 7, 京都).

報道発表等

なし

G. 知的財産権の出願・登録状況

なし

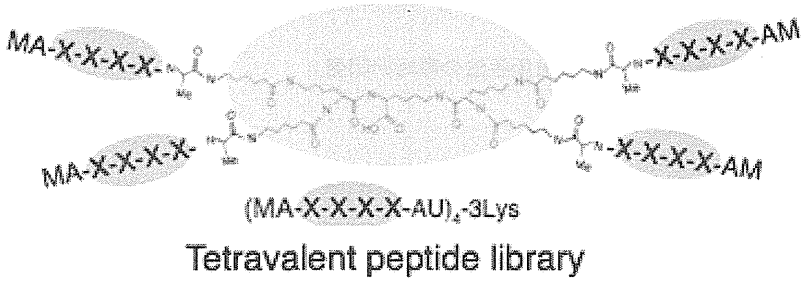

図１　多価型ペプチドライブラリーの構造
ＸはCysをのぞく１９種類のアミノ酸のミクスチャー、Ｕはスペーサーとしてのカプロン酸を示す。
Ｘの個数は標的によって最適化する。

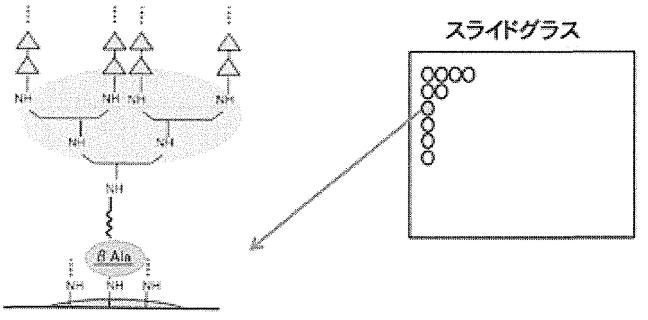

図２　多価型ペプチドライブラリーのスポット合成

様式第１９

学　会　等　発　表　実　績

委託業務題目「医薬品・医療機器の実用化促進のための評価技術手法の戦略的開発」

機関名　　国立医薬品食品衛生研究所　内藤幹彦

１．学会等における口頭・ポスター発表

発表した成果（発表題目、口頭・ポスター発表の別）	発表者氏名	発表した場所（学会等名）	発表した時期	国内・外の別
Apollonは細胞分裂初期においてスピンドルチェックポイント非依存的なcyclin Aの分解を促進する．（ポスター）	大岡伸通，内藤幹彦	日本がん分子標的治療学会第18回学術集会（仙台）	2014.6	国内
プロテアソーム阻害薬によるシガトキシン誘導性アポトーシスの抑制．（ポスター）	服部隆行，大岡伸通，内藤幹彦	日本がん分子標的治療学会第18回学術集会（仙台）	2014.6	国内
プロテアソーム阻害薬による志賀毒素誘導性細胞死の抑制．（口頭）	服部隆行，高橋美帆，大岡伸通，西川喜代孝，内藤幹彦	第18回腸管出血性大腸菌感染症研究会（京都）	2014.7	国内
SNIPER: Inducing protein degradation via recruitment to IAP. （口頭）	内藤幹彦	248th ACS National Meeting and Exposition (San Francisco, USA)	2014.8	国外
ユビキチン・プロテアソームシステムを利用したTACC3分解誘導剤によるがん細胞死の誘導．（ポスター）	大岡伸通，奥平桂一郎，柴田識人，服部隆行，内藤幹彦	第73回日本癌学会学術総会（横浜）	2014.9	国内
終止コドンのリードスルー変異によるユビキチン-プロテアソーム系を介した蛋白質の不安定化．（ポスター）	柴田識人，大岡伸通，権藤洋一，内藤幹彦	第73回日本癌学会学術総会（横浜）	2014.9	国内
ユビキチン・プロテアソームシステムを利用したTACC3分解誘導剤による癌細胞死の誘導．（横浜）	大岡伸通，永井克典，奥平桂一郎，柴田識人，服部隆行，長展生，内藤幹彦	第37回日本分子生物学会年会（横浜）	2014.11	国内
Destabilization of carboxy-teminally extended proteins encoded by stop codon read-through mutation via ubiquitin-proteasome system. （ポスター）	柴田識人，大岡伸通，櫻庭喜行，権藤洋一，内藤幹彦	Symposium for young ubiquitin researchers in Japan “New Era in the Ubiquitin Research” （京都）	2014.11	国内

SNIPER(TACC3) degrades TACC3 protein via the ubiquitin-proteasome pathway and induces apoptosis in cancer cells expressing a large amount of TACC3. (ポスター)	大岡伸通, 永井克典, 奥平桂一郎, 柴田識人, 服部隆行, 長展生, 内藤幹彦	26th EORTC-NCI-AACR Symposium on Molecular Targets and Cancer Therapeutics (Barcelona, Spain)	2014.11	国外
Protein Knockdown Targeted Destruction of Pathogenic Proteins by SNIPER Compounds. (口頭)	内藤幹彦	日本薬学会第135年会 (神戸)	2015.3	国内
ユビキチン・プロテアソームシステムを利用したTACC3分解誘導剤の開発と抗がん活性評価. (ポスター)	大岡伸通, 永井克典, 服部隆行, 奥平桂一郎, 柴田識人, 長展生, 内藤幹彦	日本薬学会第135年会 (神戸)	2015.3	国内
新規小胞輸送阻害剤による志賀毒素の細胞死誘導活性の抑制. (ポスター)	服部隆行, 高橋美帆, 椎名勇, 大橋愛美, 旦慎吾, 西川喜代孝, 内藤幹彦	日本薬学会第135年会 (神戸)	2015.3	国内
終止コドンのリードスルー変異によるユビキチン-プロテアソーム系を介した蛋白質の不安定化. (ポスター)	柴田識人, 大岡伸通, 櫻庭喜行, 権藤洋一, 内藤幹彦	日本薬学会第135年会 (神戸)	2015.3	国内

２．学会誌・雑誌等における論文掲載

掲載した論文（発表題目）	発表者氏名	発表した場所（学会誌・雑誌等名）	発表した時期	国内・外の別
Cancer cell death induced by novel small molecules degrading the TACC3 protein via the ubiquitin-proteasome pathway.	大岡伸通, 永井克典, 服部隆行, 奥平桂一郎, 柴田識人, 長展生, 内藤幹彦	Cell Death & Disease	2014.5	国外

（注１）発表者氏名は、連名による発表の場合には、筆頭者を先頭にして全員を記載すること。

（注２）本様式はexcel形式にて作成し、甲が求める場合は別途電子データを納入すること。

様式第１９

学　会　等　発　表　実　績

委託業務題目「医薬品・医療機器の実用化促進のための評価技術手法の戦略的開発」

機関名　　国立医薬品食品衛生研究所　栗原正明

１．学会等における口頭・ポスター発表

発表した成果（発表題目、口頭・ポスター発表の別）	発表者氏名	発表した場所（学会等名）	発表した時期	国内・外の別
VDR-コアクチベータ結合阻害能を有するステープルペプチドの創製．（ポスター）	川村　愛，出水庸介，三澤隆史，栗原正明	日本ケミカルバイオロジー学会第9回年会	2014．6	国内
オリゴアルギニンをベースとした細胞膜透過性ヘリカルペプチドの開発．（ポスター）	山下博子，出水庸介，三澤隆史，大庭　誠，田中正一，栗原正明	第30回日本DDS学会	2014．7	国内
エストロゲン受容体転写阻害能を有するペプチドの創製．（口頭）	長久保貴哉，出水庸介，三澤隆史，佐藤由紀子，諫田泰成，奥平桂一郎，関　祐子，内藤幹彦，栗原正明	第58回日本薬学会関東支部大会	2014．10	国内
マルチアプローチによる転写制御分子の創製．（口頭）	栗原正明	化学系シンポジウム有機化学の最前線，第58回日本薬学会関東支部大会	2014．10	国内
エストロゲン受容体転写阻害ペプチドの開発（口頭）	出水庸介，長久保貴哉，三澤隆史，佐藤由紀子，諫田泰成，奥平桂一郎，関野裕子，内藤幹彦，栗原正明：	第40回反応と合成の進歩シンポジウム	2014．11	国内
二次構造制御に基づく膜透過性ヘリカルペプチドの創製．（ポスター）	山下博子，出水庸介，三澤隆史，大庭誠，田中正一，栗原正明：	第40回反応と合成の進歩シンポジウム	2014．11	国内
アルキル基の長さに着目したエストロゲン受容体分解誘導剤の構造最適化研究．（ポスター）	加藤雅士，正田卓司，奥平桂一郎，井上英史，内藤幹彦，栗原正明	第32回メディシナルケミストリーシンポジウム	2014．11	国内

２．学会誌・雑誌等における論文掲載

掲載した論文（発表題目）	発表者氏名	発表した場所 （学会誌・雑誌等名）	発表した時期	国内・外の別
Peptides as Inhibitors of Estrogen Receptor-Mediated Transcription.	Nagakubo T, Demizu Y, Kanda Y, Misawa T, Shoda T, Okuhira K, Sekino Y, Naito M, Kurihara M.	*Bioconjugate Chem*, 25, 1921-1924	2014	国外
Amphipathic short helix-stabilized peptides with cell-membrane penetrating ability.	Yamashita H, Demizu Y, Shoda T, Sato Y, Oba M, Tanaka M, Kurihara M.	*Bioorg. Med. Chem.*, 22, 2403-2408	2014	国外
短鎖ペプチドのヘリカル構造制御と機能化	出水 庸介, 三澤 隆史, 栗原 正明,	有機合成化学協会誌, 72, 1336-1347	2014	国内

（注１）発表者氏名は、連名による発表の場合には、筆頭者を先頭にして全員を記載すること。

（注２）本様式はexcel形式にて作成し、甲が求める場合は別途電子データを納入すること。

様式第１９

学　会　等　発　表　実　績

委託業務題目「医薬品・医療機器の実用化促進のための評価技術手法の戦略的開発」

機関名　同志社大学　西川喜代孝

１．学会等における口頭・ポスター発表

発表した成果（発表題目、口頭・ポスター発表の別）	発表者氏名	発表した場所（学会等名）	発表した時期	国内・外の別
AB5型細菌毒素に対する多価型ペプチド性阻害薬の開発（口頭）	西川喜代孝	第８８回日本細菌学会総会	2015年3月	国内
異なった受容体結合部位を標的とするStx阻害薬の併用による相乗効果（ポスター）	高橋美帆、清水英子、加藤美帆子、西川喜代孝	第８８回日本細菌学会総会	2015年3月	国内
耐熱性エンテロトキシンに対するペプチド性阻害薬開発（ポスター）	近江 純平、高橋 美帆、宮坂知宏、山崎 伸二、日高 雄二、杤尾 豪人、濱端 崇、西川喜代孝	第８８回日本細菌学会総会	2015年3月	国内
新規ペプチド性コレラ毒素阻害薬のin vivoでの効果（ポスター）	雲井香保里、高橋美帆、山本洋、濱端崇、西川喜代孝	第８８回日本細菌学会総会	2015年3月	国内
ホスファチジン酸結合性を有する４価型人工ペプチドの開発（口頭）	小川莉奈、宮崎俊秀、長尾耕治郎、原雄二、佐々木善浩、秋吉一成、稲葉岳彦、小林俊彦、高橋美帆、西川喜代孝、梅田真郷	第８７回日本生化学会大会	2014年10月	国内
受容体結合部位特異的Stx阻害薬の組み合わせによる阻害効果の増強（口頭）	高橋美帆、清水英子、加藤美帆子、西川喜代孝	第１８回腸管出血性大腸菌感染症研究会	2014年7月	国内

２．学会誌・雑誌等における論文掲載

掲載した論文（発表題目）	発表者氏名	発表した場所（学会誌・雑誌等名）	発表した時期	国内・外の別
Identification of a wide range of motifs inhibitory to Shiga toxin by affinity-driven screening of customized divalent peptides synthesized on a membrane.	Kato M., Watanabe-Takahashi M., Shimizu E., and Nishikawa K.	*Appl. Environ. Microbiol.*, 81: 1092-1100.	2015.1	国外

（注１）発表者氏名は、連名による発表の場合には、筆頭者を先頭にして全員を記載すること。

（注２）本様式はexcel形式にて作成し、甲が求める場合は別途電子データを納入すること。

OPEN

Citation: Cell Death and Disease (2014) 5, e1513; doi:10.1038/cddis.2014.471

www.nature.com/cddis

Cancer cell death induced by novel small molecules degrading the TACC3 protein via the ubiquitin–proteasome pathway

N Ohoka[1], K Nagai[2], T Hattori[1], K Okuhira[1], N Shibata[1], N Cho[2] and M Naito*[,1]

The selective degradation of target proteins with small molecules is a novel approach to the treatment of various diseases, including cancer. We have developed a protein knockdown system with a series of hybrid small compounds that induce the selective degradation of target proteins via the ubiquitin–proteasome pathway. In this study, we designed and synthesized novel small molecules called SNIPER(TACC3)s, which target the spindle regulatory protein transforming acidic coiled-coil-3 (TACC3). SNIPER(TACC3)s induce poly-ubiquitylation and proteasomal degradation of TACC3 and reduce the TACC3 protein level in cells. Mechanistic analysis indicated that the ubiquitin ligase APC/C^{CDH1} mediates the SNIPER(TACC3)-induced degradation of TACC3. Intriguingly, SNIPER(TACC3) selectively induced cell death in cancer cells expressing a larger amount of TACC3 protein than normal cells. These results suggest that protein knockdown of TACC3 by SNIPER(TACC3) is a potential strategy for treating cancers overexpressing the TACC3 protein.
Cell Death and Disease (2014) **5,** e1513; doi:10.1038/cddis.2014.471; published online 6 November 2014

Inhibitors of microtubule polymerization or depolymerization such as *Vinca* alkaloids and taxanes, respectively, are widely used as anti-cancer drugs. They arrest cancer cells, inducing mitotic catastrophe and cancer cell death. However, these drugs also affect microtubule function in non-dividing cells and have serious side effects, such as peripheral neuropathy, which limit their utility.[1] Recently, inhibitors of spindle-regulatory proteins, such as mitotic kinases (Aurora kinases and Polo-like kinases) and a motor protein (Eg5/Ksp) have attracted considerable attention, but they have not been developed clinical use yet.[2,3]

Transforming acidic coiled-coil-3 (TACC3) is another spindle-regulatory protein.[4,5] During mitosis, TACC3 localizes to the mitotic spindle and has a critical role in spindle assembly, chromosomal function and mitotic progression.[6–11] Studies using microarray and immunohistochemical analysis showed that TACC3 is overexpressed in many human cancers, including ovarian cancer, breast cancer, squamous cell carcinoma and lymphoma.[12–14] Depletion of TACC3 results in chromosome alignment defects, multi-polar spindle formation, mitotic cell death and/or a postmitotic cell cycle arrest.[15–20] Additionally, conditional disruption of TACC3 has been shown to regress thymic lymphomas in p53-deficient mice without inducing any overt abnormalities in normal tissues.[21] These findings suggest that TACC3 is a molecular target for anti-cancer drug discovery.

The development of a strategy for the selective degradation may be a useful approach to the discovery of novel drugs. Based on the ubiquitin–proteasome system (UPS), we have devised a protein knockdown system for inducing the selective degradation of target proteins by using specifically designed hybrid small compounds.[22–29] These compounds, which we have termed SNIPER (Specific and Non-genetic IAP-dependent Protein ERaser), are composed of two different ligands connected by a linker; one is a ligand for cellular inhibitor of apoptosis protein 1 (cIAP1) and the other a ligand for the target protein. Accordingly, SNIPER is expected to crosslink the ubiquitin–ligase cIAP1 and the target protein in the cells, thereby inducing ubiquitylation and, ultimately, proteasomal degradation of the target protein. To date, we have constructed SNIPERs that target cellular retinoic acid binding protein-II (CRABP-II) and nuclear receptors such as estrogen receptor α (ERα) for degradation.[22–28] In this study, we designed and synthesized novel SNIPERs targeting TACC3, that is, SNIPER(TACC3)s, that induce proteasomal degradation of the TACC3 protein. We also show that cancer cells expressing a large amount of the TACC3 protein readily undergo cell death as the result of SNIPER(TACC3) treatment.

Results

Effect of SNIPER(TACC3) on TACC3 protein expression. We designed and synthesized the SNIPER(TACC3) to target the TACC3 protein for degradation (Figure 1a). The synthesis and structural data on SNIPER(TACC3)-1 and -2 are presented in Materials and Methods section and Supplementary Information.

[1]Division of Biochemistry and Molecular Biology, National Institute of Health Science, Kamiyoga, Setagaya-ku, Tokyo 158-8501, Japan and [2]Medicinal Chemistry Research Laboratories, Pharmaceutical Research Division, Takeda Pharmaceutical Co. Ltd., 26-1, Muraoka-Higashi 2-chome, Fujisawa, Kanagawa 251-0012, Japan
*Corresponding author: M Naito, Division of Biochemistry and Molecular Biology, National Institute of Health Science, 1-18-1 Kamiyoga, Setagaya-ku, Tokyo 158-8501, Japan. Tel: +81 3 3700 9428; Fax: +81 3 3707 6950; E-mail: miki-naito@nihs.go.jp
Abbreviations: TACC3, transforming acidic coiled-coil-3; UPS, ubiquitin–proteasome system; SNIPER, specific and non-genetic IAP-dependent protein eraser; cIAP1, cellular inhibitor of apoptosis protein 1; CRABP-II, cellular retinoic acid binding protein-II; ERα, estrogen receptor α; Me-BS, methyl-bestatin; PEG, polyethylene glycol; siRNA, small interfering RNA; APC/C, anaphase-promoting complex/cyclosome; 4-OHT, 4-hydroxy tamoxifen; ROS, reactive oxygen species; PI, propidium iodide
Received 09.6.14; revised 22.9.14; accepted 24.9.14; Edited by M Agostini

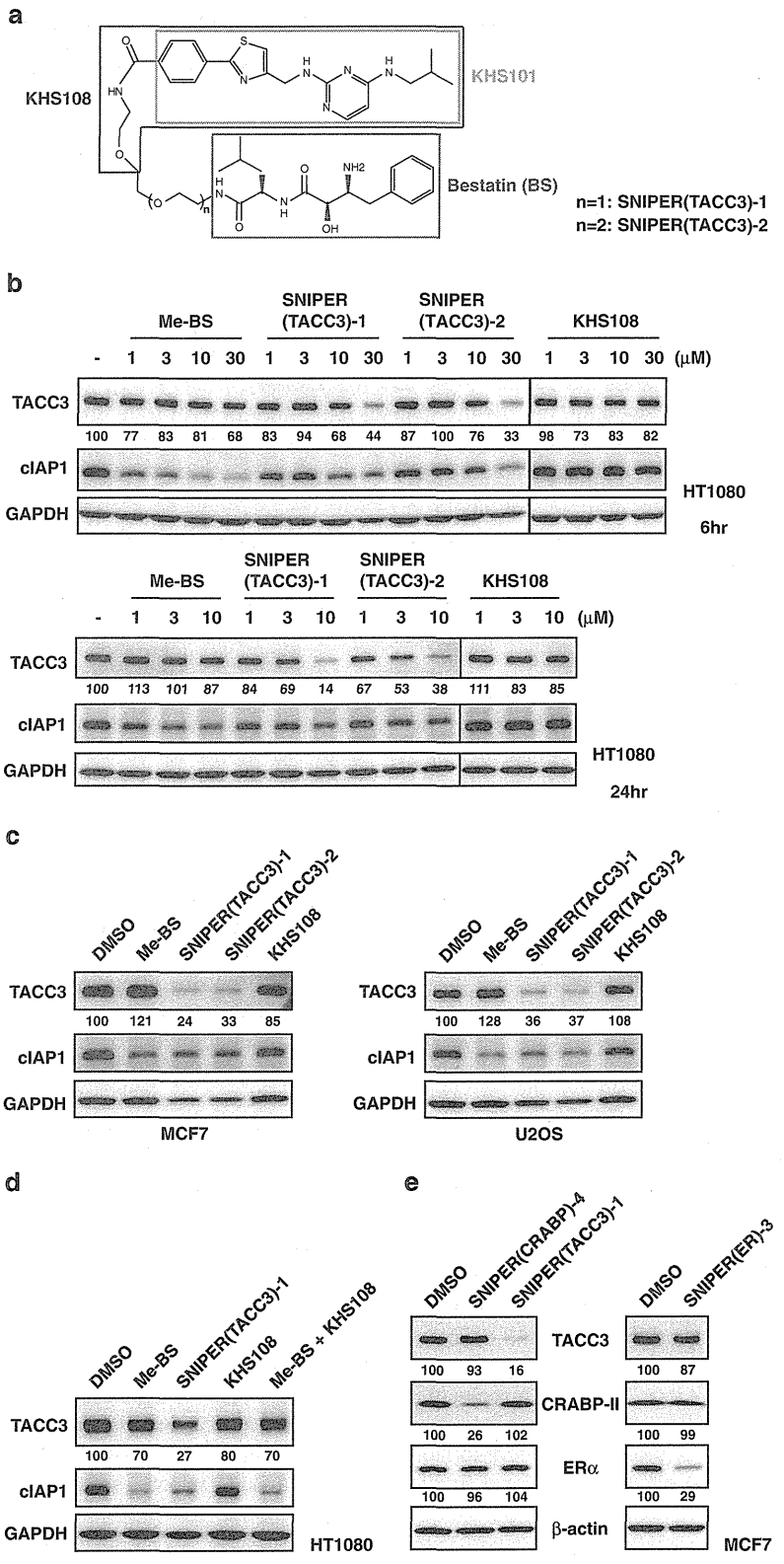

Figure 1 SNIPER(TACC3) decreases the TACC3 protein level. (**a**) Chemical structure of SNIPER(TACC3). (**b**) HT1080 cells were treated with the indicated concentration of Me-BS, SNIPER(TACC3)-1, SNIPER(TACC3)-2 or KHS108 for 6 h (upper panels) or 24 h (lower panels). (**c**) MCF7 and U2OS cells were treated with 30 μM of Me-BS, SNIPER (TACC3)-1, SNIPER(TACC3)-2 or KHS108 for 6 h. (**d**) HT1080 cells were treated with 30 μM of Me-BS, SNIPER(TACC3)-1, KHS108 or Me-BS plus KHS108 for 6 h. (**e**) MCF7 cells were treated with 10 μM of SNIPER(TACC3)-1 or SNIPER(CRABP)-4 for 6 h (left panels), or cells precultured in the media containing estrogen-depleted serum were treated with 10 μM of SNIPER(ER)-3 for 9 h (right panels). (**b–e**) Whole-cell lysates were analyzed using western blotting with the indicated antibodies. The numbers below the protein panels represent the protein level relative to control (dimethyl sulfoxide (DMSO)), which was normalized by glyceraldehyde 3-phosphate dehydrogenase (GAPDH) or β-actin

When human fibrosarcoma HT1080 cells were treated with graded concentrations of SNIPER(TACC3)-1 or -2, the TACC3 level was significantly decreased by these compounds at 30 μM for 6 h and at 10 μM for 24 h (Figure 1b). However, methyl-bestatin (Me-BS) or KHS108 marginally reduced the TACC3 protein level under the same condition. SNIPER(TACC3)s also decreased the cIAP1 level, although the effect was less than Me-BS, suggesting that the SNIPER(TACC3)s simultaneously induces auto-ubiquitylation and proteasomal degradation of cIAP1, as observed with other SNIPERs.[22,28] Similar results were obtained in human breast adenocarcinoma MCF7 or human osteosarcoma U2OS cells when the cells were treated with 30 μM of SNIPER(TACC3)s for 6 h (Figure 1c). Combination treatment with Me-BS and KHS108 did not decrease the TACC3 protein level, indicating that linking the two ligands into a single molecule is critically important for the reduction of the TACC3 protein (Figure 1d). Additionally, we examined the target specificity of the SNIPERs we have developed. SNIPER(TACC3), SNIPER(CRABP) and SNIPER(ER) reduced the level of respective target proteins without reducing the other proteins (Figure 1e), indicating the specificity of SNIPERs on the degradation of the target proteins.

Ubiquitylation and proteasomal degradation of TACC3 protein by SNIPER(TACC3). To investigate whether the reduction of the TACC3 protein by SNIPER(TACC3) is mediated by proteasomal degradation, HT1080 cells were co-treated with SNIPER(TACC3) and the proteasome inhibitor MG132. As shown in Figure 2a, the decrease in the TACC3 protein by SNIPER(TACC3)s was abrogated by MG132, indicating that SNIPER(TACC3)s reduce TACC3 protein by a proteasome-dependent mechanism.

We next examined the effect of SNIPER(TACC3) on the ubiquitylation of TACC3. HT1080 cells were transiently co-transfected with the expression vectors of Flag-tagged TACC3 and HA-tagged ubiquitin and then treated with SNIPER (TACC3)-1 or control compounds in the presence of MG132. The cell lysates were heat-denatured to dissociate non-covalently bound proteins, then re-natured and immunoprecipitated with anti-FLAG (TACC3) antibody. The immunoprecipitates were subsequently analyzed by western blotting with an anti-HA (ubiquitin) to detect ubiquitylated TACC3 proteins (Figure 2b, left panels). SNIPER(TACC3)-1 treatment, but not Me-BS or KHS108, shifted the smear bands of the poly-ubiquitylated TACC3 protein to a more slowly migrating position (near the top of gel), indicating that SNIPER(TACC3) induces a higher level of poly-ubiquitylation of the TACC3 protein. We carried out a similar experiment with an antibody specific to K48-linked ubiquitin and observed a more conspicuous enhancement of K48-polyubiquitylated TACC3 protein by SNIPER(TACC3), but not by Me-BS nor KHS108 (Figure 2b, right panels). These results indicate that SNIPER(TACC3)s induce poly-ubiquitylation and proteasomal degradation of TACC3 proteins within cells.

SNIPER(TACC3)-induced degradation of TACC3 protein requires APC/C^{CDH1}. As SNIPER(TACC3) is designed to crosslink the ubiquitin ligase cIAP1 to the TACC3 protein, we reasoned that the TACC3 protein is degraded subsequent to cIAP1-mediated ubiquitylation. To examine whether cIAP1 is actually involved in the SNIPER (TACC3)-induced TACC3 degradation, we pretreated the cells with small interfering RNA (siRNA) against cIAP1 and measured the reduction of TACC3 protein by SNIPER(TACC3)s. We used three different siRNAs against cIAP1, and they all efficiently downregulated the cIAP1 protein level. Unexpectedly, however, the downregulation of the cIAP1 protein did not abrogate the reduction in the TACC3 protein by SNIPER(TACC3)s (Figure 3a). This result suggests that the TACC3 protein is ubiquitylated by a different ubiquitin ligase than cIAP1 in the SNIPER(TACC3)-treated cells.

As an inherent component in the degradation machinery, the anaphase-promoting complex/cyclosome in complex with CDH1 (APC/C^{CDH1}) has been shown to ubiquitylate TACC3 proteins during late mitosis.[30] To examine whether APC/C^{CDH1} participates in the SNIPER(TACC3)-dependent degradation of the TACC3 protein, we downregulated key components of APC/C^{CDH1} by the siRNAs. Knockdown of CDH1, a substrate-recognition subunit for TACC3, completely abolished the reduction of TACC3 protein by SNIPER(TACC3)-1 treatment, while the knockdown of CDC20, another substrate-recognition subunit in APC/C for different proteins,[31] scarcely attenuated the TACC3 reduction (Figure 3b). In addition, knockdown of APC11, a RING H2 subunit recruiting E2 enzyme,[31] and APC3, a core component of APC/C, also abrogated the TACC3 reduction by SNIPER(TACC3). We repeated the experiments with three different siRNAs against CDH1, and the abrogation of TACC3 protein knockdown was confirmed (Figure 3c). These results indicate that APC/C^{CDH1} is required for the SNIPER(TACC3)-induced degradation of the TACC3 protein.

To confirm the physical interaction of SNIPER(TACC3) and APC/C^{CDH1}, we performed a thermal shift assay that is based on the biophysical principle of ligand-induced change of thermal sensitivity of target proteins[32] (Figure 4a). Multiple aliquots of the cell lysates were mixed with each compounds (SNIPER (TACC3)-1, Me-BS or KHS108) and heated to graded temperatures. After cooling, the lysates were centrifuged to precipitate unfolded proteins, and the supernatants were analyzed by western blotting. The thermal sensitivity of APC/C^{CDH1} components (APC3, APC11 and CDH1) were changed by addition of SNIPER(TACC3)-1, but not by Me-BS and KHS108. On the other hand, the thermal sensitivity of CDC20 was not affected by these compounds. These results indicate the physical interaction of SNIPER(TACC3) and APC/C^{CDH1}.

Next we examined whether SNIPER(TACC3) treatment increases the interaction between TACC3 and APC/C^{CDH1} by crosslinking these proteins. As TACC3 inherently interacts with APC/C^{CDH1}, we tried to discriminate the SNIPER (TACC3)-mediated interaction of these proteins by the following procedure (Figure 4b). HT1080 cells were transiently co-transfected with the expression vectors of Flag-TACC3 and Myc-CDH1 and then treated with MG132 in the presence or absence of SNIPER(TACC3)-1. The cell lysates were immunoprecipitated with anti-FLAG (TACC3) antibody, and the immunoprecipitates were eluted with an excess amount of either KHS108 or Me-BS to detect the APC/C^{CDH1} components that had associated with TACC3 depending on SNIPER(TACC3) (Supplementary Figure S1). Figure 4c shows a significant increase of Myc-CDH1 and endogenous APC3 in the fractions eluted with KHS108 and Me-BS but not with 4-hydroxy tamoxifen (4-OHT) as a control compound. Me-BS eluted the proteins probably by disturbing the binding of SNIPER(TACC3) to APC/C^{CDH1}. These results strongly suggest that there are

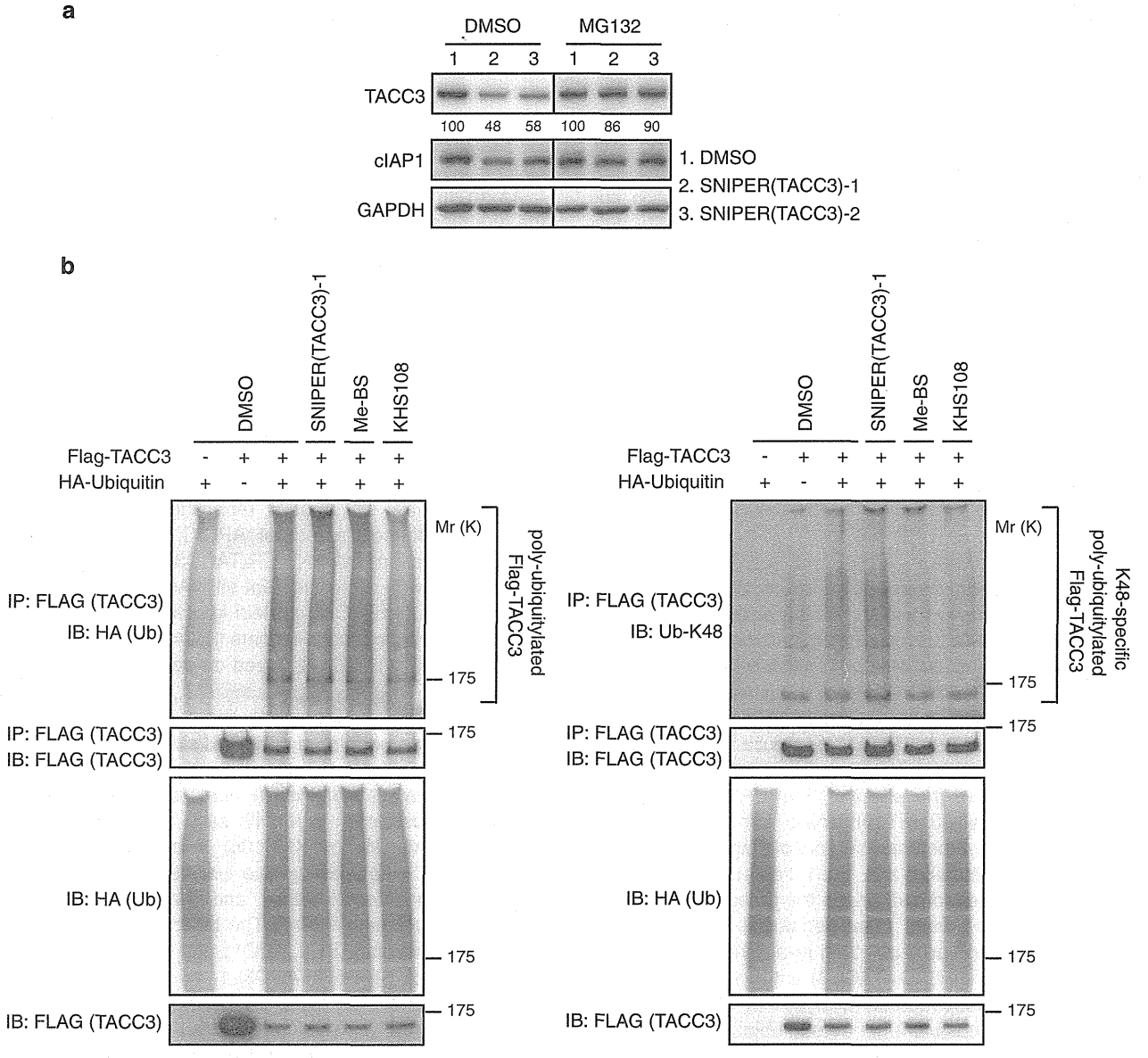

Figure 2 SNIPER(TACC3) induces ubiquitylation and proteasomal degradation of TACC3. (**a**) HT1080 cells were treated with 30 μM of SNIPER(TACC3)-1 or -2 in the presence or absence of 25 μM of MG132 for 4 h. Whole-cell lysates were analyzed using western blotting with the indicated antibodies. The numbers below the TACC3 panels represent the TACC3 level relative to the respective control normalized by glyceraldehyde 3-phosphate dehydrogenase (GAPDH). (**b**) HT1080 cells were co-transfected with the expression vector of Flag-TACC3 and/or HA-ubiquitin. After 40 h, cells were treated with the indicated compounds in the presence of 25 μM of MG132 for 3 h. Cells were lysed, and Flag-TACC3 was immunoprecipitated with an anti-FLAG antibody. The ubiquitylated TACC3 was detected with an anti-HA antibody (left panels) or an antibody specific to K48-linked ubiquitin (right panels). DMSO, dimethyl sulfoxide; IB, immunoblot; IP, immunoprecipitation

two types of interaction between TACC3 and APC/C^{CDH1}: one is an inherent interaction independent of SNIPER(TACC3) (Supplementary Figure S1A), and the other is a SNIPER (TACC3)-mediated interaction (Supplementary Figure S1B). SNIPER(TACC3) is likely to increase the amount of TACC3 associated with APC/C^{CDH1} via the second mechanism.

As the SNIPER(TACC3) interacts with APC/C^{CDH1}, it is possible that it directly activates APC/C^{CDH1} and promotes the degradation of many target proteins. Therefore, we explored the possibility that SNIPER(TACC3) may facilitate the degradation of a variety of proteins ubiquitylated by APC/C^{CDH1}. As cyclin B and CDC20 are known to be ubiquitylated by APC/C^{CDH1},[33] the turnover of these proteins was examined after SNIPER(TACC3) treatment. The result showed that TACC3 was scarcely degraded until 6 h in control cells, but rapidly degraded in the SNIPER(TACC3)-treated cells, with a half-life of approximately 5 h (Figure 5). However, the degradation of cyclin B and CDC20 was unaffected by SNIPER(TACC3)-1 treatment. This result suggests that SNIPER(TACC3) specifically facilitates degradation of the TACC3 protein. We also investigated cell cycle distribution of HT1080 cells treated with SNIPER(TACC3)-1 for 4 h (Supplementary Figure S2). The result showed that SNIPER(TACC3) did not affect the cell cycle distribution, suggesting that the degradation of TACC3 by SNIPER (TACC3)-1 is not due to arresting cells in a certain cell cycle phase where the protein is preferentially degraded.

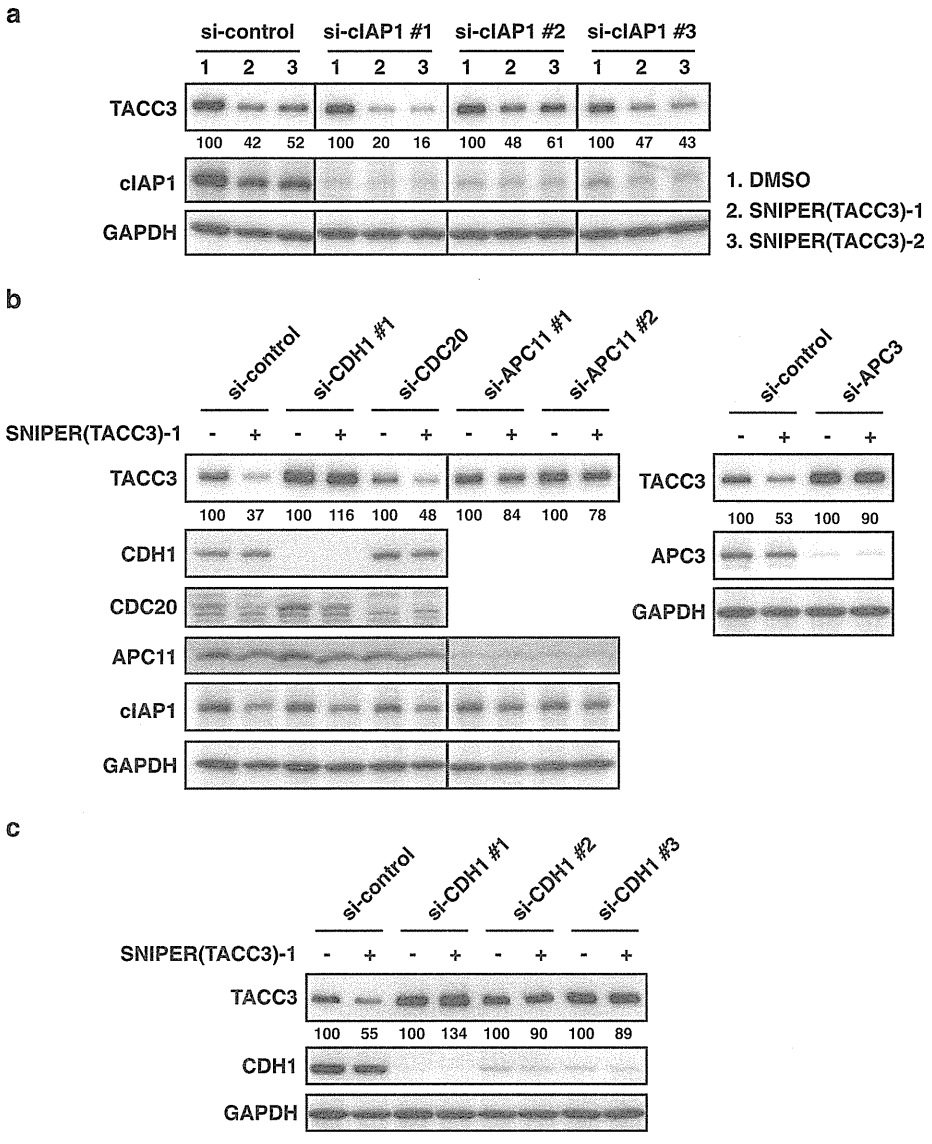

Figure 3 APC/C^{CDH1} mediates SNIPER-induced TACC3 reduction. (**a–c**) HT1080 cells were transfected with the indicated siRNA for 40 h and treated with 30 μM of SNIPER (TACC3)-1 for 4 h. Whole-cell lysates were analyzed using western blotting with the indicated antibodies. The numbers below the TACC3 panels represent the TACC3 level relative to the respective control normalized by glyceraldehyde 3-phosphate dehydrogenase (GAPDH). DMSO, dimethyl sulfoxide

Selective cytotoxicity of SNIPER(TACC3) against cancer cells. In some cancer cell lines, depletion of TACC3 induces postmitotic cell cycle arrest or mitotic cell death.[15–19] TACC3 deletion was also shown to result in a massive apoptotic regression of mouse thymic lymphoma *in vivo* without any overt abnormalities in normal tissues.[21] Therefore, we tested the effect of SNIPER(TACC3) on the cell viability of cancer cells. HT1080 and MCF7 cells were treated with Me-BS, KHS108, their combination or SNIPER (TACC3)-1 for 48 h, and cell viability was determined. SNIPER (TACC3) at $\geq 10\,\mu$M efficiently killed the cancer cells (Figure 6a), which is consistent with the protein knockdown activity under long-term (24 h) treatment (Figure 1b). On the other hand, individual or combined treatment with Me-BS and KHS108 exhibited mild effects on the cell viability up to 30 μM. In line with this, SNIPER(TACC3)-1 at 10 μM, but not Me-BS, KHS108 or their combination, induced caspase-3 activation and PARP cleavage in the cells, suggesting SNIPER(TACC3) induces apoptotic cell death (Figure 6b). We also examined the effects of SNIPER(TACC3) on the viability of other cancer cell lines and normal cells. Figure 6c shows that the cell viability was greatly reduced by SNIPER(TACC3)-1 and -2 in human cancer cells but minimally in normal human fibroblasts. Selective induction of apoptosis in cancer cells by SNIPER(TACC3) was confirmed by Annexin V/propidium iodide (PI) staining (Supplementary Figure S3) and flow cytometric analysis (Supplementary Figure S4). To understand the mechanism behind the selective toxicity of SNIPER(TACC3) against cancer cells, we compared the level of TACC3 protein. Figure 6d shows that the expression level of TACC3 protein in cancer cells was much higher than that in normal cells. Depletion of TACC3 by siRNA showed only mild effect on cell cycle distribution and cell viability in these cell lines (Supplementary Figure S5). However, when SNIPER (TACC3)-induced degradation of TACC3 protein was abrogated by siRNA against APC/C^{CDH1} components (Figures 3b and c), SNIPER(TACC3)-induced cancer cell death was seriously

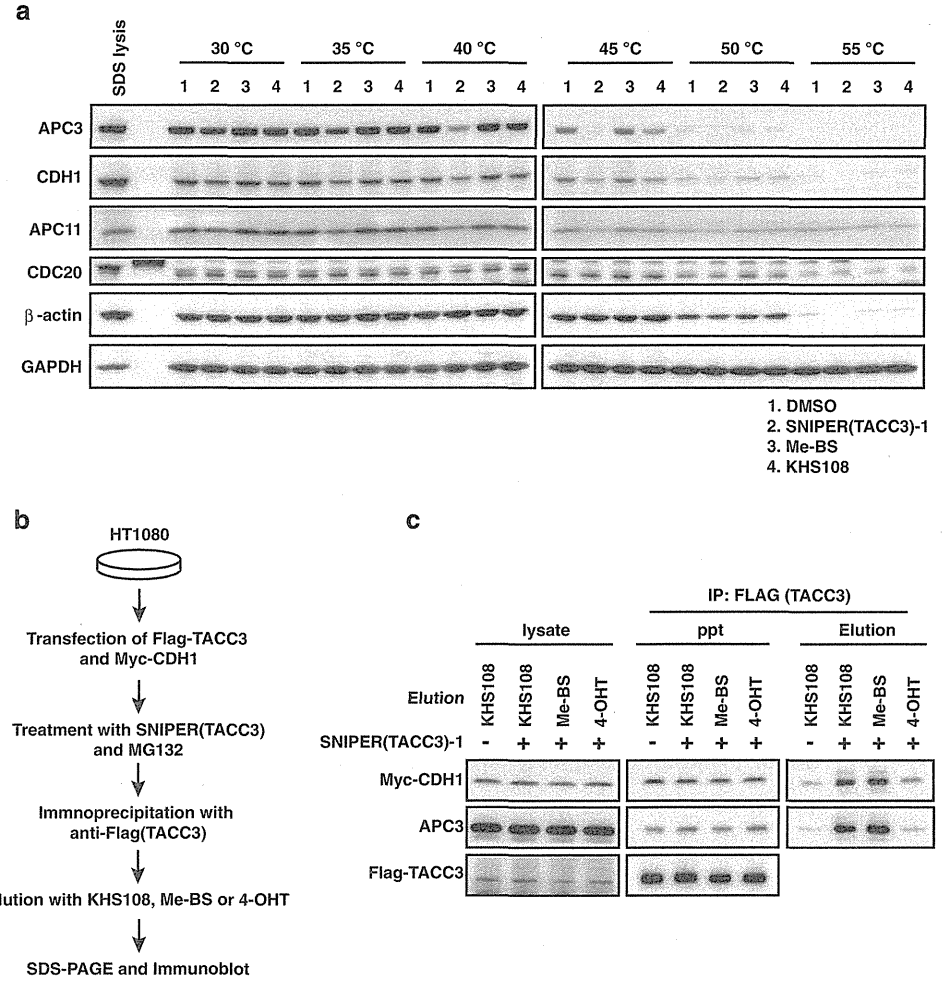

Figure 4 SNIPER(TACC3) physically interacts with APC/C^{CDH1} and increases the TACC3–APC/C^{CDH1} interaction. (**a**) Cell lysates were mixed with 100 μM of SNIPER (TACC3)-1, Me-BS or KHS108 and analyzed by a thermal shift assay. (**b**) Scheme of the experimental procedure to detect the SNIPER(TACC3)-mediated interaction of TACC3 and APC/C^{CDH1}. (**c**) HT1080 cells were co-transfected with the expression vector of Flag-TACC3 and Myc-CDH1. After 40 h, cells were treated with 25 μM of MG132 in the presence or absence of 30 μM of SNIPER(TACC3)-1 for 3 h. Cells were lysed in immunoprecipitated (IP) lysis buffer and Flag-TACC3 was IP with an anti-FLAG antibody. The precipitates were eluted with 2 mM of KHS108, Me-BS or 4-OHT. Total cell lysates, immunoprecipitates after elution and eluted fractions were western blotted with the indicated antibodies. DMSO, dimethyl sulfoxide; Elution, eluted fraction; lysate, total lysate; ppt, immunoprecipitate after elution; SDS-PAGE, sodium dodecyl sulfate-polyacrylamide gel electrophoresis

suppressed (Supplementary Figure S6). These results suggest that SNIPER(TACC3) selectively kills cancer cells expressing a large amount of the TACC3 protein, and the degradation of TACC3 protein has an important role in the SNIPER(TACC3)-induced cancer cell death.

Discussion

Protein knockdown with SNIPER technology selectively degrades target proteins by small molecules composed of two ligands, one against cIAP1 and the other against a target protein. Theoretically, this method enables the induction of a rapid degradation of a target even if it is a long-lived protein, which stands in contrast with the repression of protein synthesis by siRNA and antisense oligonucleotides that require a longer time to achieve efficient knockdown. We have developed a series of SNIPER compounds targeting a variety of proteins, including CRABP-II and ERα.[22–28] These SNIPERs are designed to induce cIAP1-mediated ubiquitylation and proteasomal degradation of the target proteins, and they actually reduce the target proteins by the expected mechanism.

In this study, on the basis of our previous success, we designed and synthesized SNIPER(TACC3) to target TACC3 protein for degradation. The SNIPER(TACC3) induces proteasomal degradation of the TACC3 protein in the cells, as intended. Unexpectedly, however, cIAP1 is not involved in the SNIPER(TACC3)-mediated protein knockdown of the TACC3 protein. Instead, APC/C^{CDH1} has an important role in the degradation of the TACC3 induced by SINPER(TACC3). As APC/C^{CDH1} is a physiological E3 ligase for TACC3[30] and SNIPER(TACC3) interacts with APC/C^{CDH1}, it is possible that SNIPER(TACC3) non-specifically activates APC/C^{CDH1} in order to facilitate the ubiquitylation and degradation of many different proteins. However, this is not the case, because degradation of cyclin B and CDC20, both of which are substrates for APC/C^{CDH1}-mediated ubiquitylation as well, were not facilitated by SNIPER(TACC3). A thermal shift assay

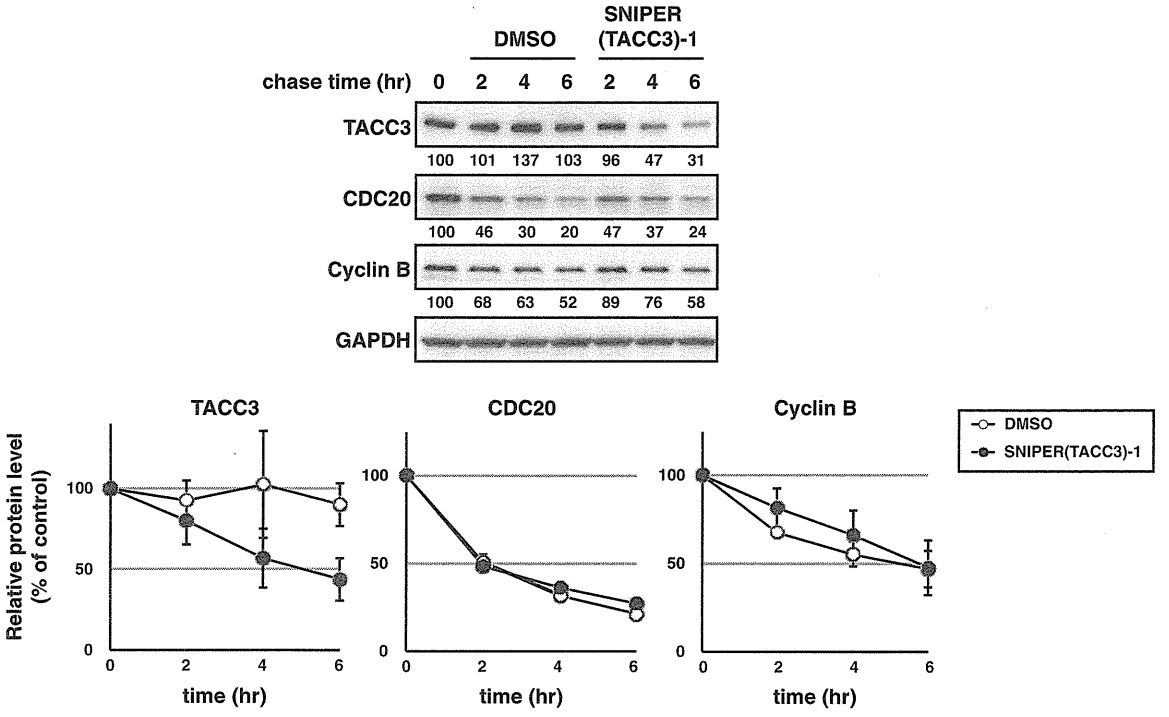

Figure 5 Turnover rate of APC/C substrate proteins. HT1080 cells were treated with 10 μg/ml of cycloheximide in the presence or absence of 30 μM of SNIPER(TACC3)-1 for the indicated periods. Whole-cell lysates were analyzed using western blotting with the indicated antibodies (top). The expression levels of TACC3, CDC20 and Cyclin B were normalized by glyceraldehyde 3-phosphate dehydrogenase (GAPDH), and the relative levels compared with time 0 were evaluated. The graphs are the means ± S.D. of a representative experiment performed in triplicate (bottom). DMSO, dimethyl sulfoxide

and co-immunoprecipitation followed by elution with individual ligands (KHS108 and Me-BS) (Figure 4) suggest that SNIPER (TACC3) crosslinks TACC3 and APC/C^{CDH1}, thereby increasing the interaction of these proteins (Supplementary Figure S1). Thus, unlike other SNIPERs that induce cIAP1-mediated ubiquitylation of target proteins, SNIPER(TACC3) induces APC/C^{CDH1}-mediated ubiquitylation of the TACC3 protein. In all cases, the ubiquitylated proteins were subjected to proteasomal degradation, resulting in a reduction of the target.

TACC3 has a pivotal role on the regulation of spindle formation. When the TACC3 protein is depleted by siRNA or genetic ablation, cell lines show mitotic or postmitotic arrest and occasionally undergo apoptosis.[7,15,16,19,20] However, as thus far examined with SNIPER(TACC3)s, we did not observe any mitotic arrest but rather cell death via apoptosis. This may be due to an insufficient reduction of the TACC3 protein and/or simultaneous reduction of anti-apoptotic cIAP1 protein by SNIPER(TACC3) treatment. It is also possible that SNIPER (TACC3) additionally affect a cellular function related to cell death. In the case of SNIPER(ER), there is a robust production of reactive oxygen species (ROS) after ERα degradation that results in necrotic cell death accompanied by the release of HMGB1 from the cells.[28] SNIPER(TACC3), however, does not induce a robust ROS production in cells.

One of the interesting feature of SNIPER(TACC3) is the ability to induce apoptosis selectively in cancer cells expressing large amounts of TACC3 protein. As TACC3 level is higher in actively dividing cells, SNIPER(TACC3) might selectively kill cancer cells that are more actively proliferating than non-tumor cells. Degradation of TACC3 seems to have an important role in the SNIPER(TACC3)-induced apoptosis, because down-regulation of APC/C^{CDH1}-components by siRNA abrogates the SNIPER(TACC3)-induced TACC3 degradation (Figure 3), and suppresses cell death (Supplementary Figure S6), though TACC3 depletion by siRNA is not enough to induce cell death in these cancer cells (Supplementary Figure S5),

Recently, TACC3 has attracted increasing attention as a target for cancer therapy,[21,34–41] and inhibitors of TACC3 have been reported to possess anti-tumor activity.[42] As SNIPER (TACC3) exhibits selective toxicity to cancer cells aberrantly expressing large amount of the TACC3 protein as compared with normal cells, protein knockdown is a strategy for disrupting TACC3 function in cancer cells.

Materials and Methods

Design and synthesis of SNIPER(TACC3)-1 and -2. The small-molecule KHS101 and its derivative KHS108 have been reported to interact with the TACC3 protein.[43] Accordingly, KHS101 and bestatin were used as TACC3 and cIAP1 ligands, respectively. We designed the hybrid molecules SNIPER(TACC3)-1 and -2 in which KHS108 is linked to bestatin via a linker having a different polyethylene glycol (PEG) unit (Figure 1a). The attachment point of KHS108 to the PEG linker was determined at the end of the methoxyethylaminocarbonyl group, which does not affect the neuronal differentiation activities of KHS101 derivatives according to the literature.[43]

The chemical synthesis and physicochemical data on SNIPER(TACC3)-1 and -2 are provided in the Supplementary Information.

Plasmids. The cDNA encoding human TACC3 was amplified by PCR from HepG2 cDNA and cloned into a pCMV5-FLAG expression vector. The correct cDNA sequence was confirmed. pcDNA3-Myc-CDH1 was described previously.[44]

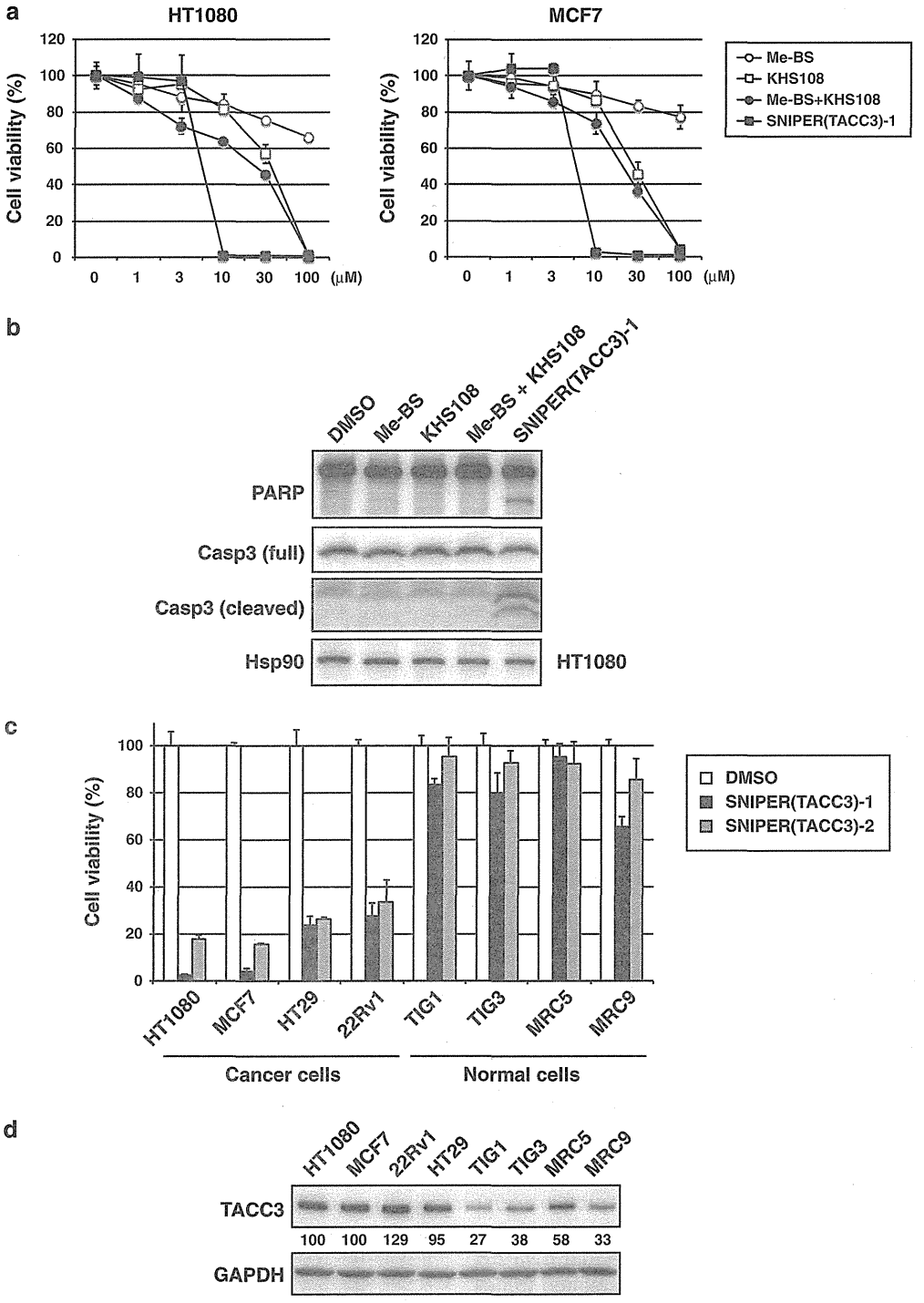

Figure 6 SNIPER(TACC3) selectively induces cancer cell death expressing a large amount of the TACC3 protein. (**a** and **c**) Cells were treated with the indicated compounds for 48 h, and cell viability was measured by WST-8 cell proliferation assay. The graphs show the means ± S.D. of a representative experiment performed in triplicate. (**b**) Cells were treated with 10 μM of the indicated compounds for 24 h, and the whole-cell lysates were analyzed by western blotting with the indicated antibodies. (**d**) Whole-cell lysates from exponentially growing cells were analyzed by western blotting. The numbers below the TACC3 panel show the relative level of TACC3 compared with HT1080 cells normalized by glyceraldehyde 3-phosphate dehydrogenase (GAPDH). DMSO, dimethyl sulfoxide

Cell culture and transfection. Human fibrosarcoma HT1080, human osteosarcoma U2OS, human colon adenocarcinoma HT29 and human fetal lung fibroblasts TIG1, TIG3, MRC5 and MRC9 were maintained in Dulbecco's modified Eagle's medium supplemented with 10% fetal bovine serum (FBS) and 100 μg/ml of kanamycin. In some experiments, MCF7 cells were precultured in the media containing estrogen-depleted serum as previously described.[28] Human breast adenocarcinoma MCF7 and human prostate carcinoma 22Rv1 were maintained in RPMI 1640 medium containing 10% FBS and 100 μg/ml of kanamycin. HT1080 cells were transiently transfected with gene-specific short interfering RNA (siRNA) or negative control siRNA (QIAGEN, Valencia, CA, USA) using lipofectamine RNAi MAX reagent (Invitrogen, Tokyo, Japan). The siRNA sequences used in this study were: human cIAP1-1 (5′-UCUAGAGCAGUUGAAGACAUCUCUU-3′); cIAP1-2

(5′-GCUGUAGCUUUAUUCAGAAUCUGGU-3′); cIAP1-3 (5′-GGAAAUGCUGCGG CCAACAUCUUCA-3′); CDH1-1 (5′-GGAUUAACGAGAAUGAGAA-3′); CDH1-2 (5′-UGAGAAGUCUCCCAGUCAG-3′); CDH1-3 (5′-GCACGGAGACCGCUUCAUC-3′); CDC20 (5′-GUCCCCCCGGAAACCCACC-3′); APC11-1 (5′-GGUGAAGAUUAAGU GCUGG-3′); APC11-2 (5′-CGAUGAGAACUGUGGCAUC-3′); and APC3 (5′-GGAA AUAGCCGAGAGGUAA-3′).

Western blotting. Cells were lysed with SDS lysis buffer (0.1 M Tris-HCl at pH 8.0, 10% glycerol, 1% SDS) and boiled for 10 min. The protein concentration was measured by the BCA method (Pierce, Rockford, IL, USA), and the lysates containing an equal amount of protein were separated by SDS-PAGE, transferred to PVDF membranes (Millipore, Darmstadt, Germany) for western blotting using the appropriate antibodies. The immunoreactive proteins were visualized using the Immobilon Western chemiluminescent HRP substrate (Millipore), and light emission was quantified with a LAS-3000 lumino-image analyzer (Fuji, Tokyo, Japan). The antibodies used in this study were: anti-TACC3 rabbit monoclonal antibody (mAb) (Cell Signaling Technology, Danvers, MA, USA; 8069), anti-TACC3 rabbit polyclonal antibody (pAb) (Santa Cruz, Dallas, TX, USA; sc-22773), anti-cIAP1 goat pAb (R&D systems, Minneapolis, MN, USA; AF8181), anti-GAPDH pAb (Santa Cruz, sc-25778 HRP), anti-CDH1 mouse mAb (Calbiochem, La Jolla, CA, USA; Ab-2), anti-CDC20 rabbit pAb (Santa Cruz, sc-8358), anti-APC11 rabbit pAb (Acris, San Diego, CA, USA; R1503), anti-APC3 mouse mAb (Santa Cruz, sc-13154), anti-cyclin B (Santa Cruz, sc-245), anti-PARP rabbit mAb (Cell Signaling Technology, 9532), anti-caspase-3 rabbit pAb (Santa Cruz, sc-7148) and anti-Hsp90 mouse mAb (BD Transduction, San Jose, CA, USA; 610419), anti-CRABP-II rabbit pAb (Abcam, Cambridge, UK; ab72099), anti-ERα rabbit mAb (Cell Signaling Technology, 8644), and anti-β-actin mouse mAb (Sigma, St. Louis, MO, USA; A2228).

Ubiquitylation assay. HT1080 cells were transfected with pCMV5-FLAG-TACC3 and pcDNA3-HA-ubiquitin for 40 h The cells were then incubated with the indicated compounds in the presence of MG132 (25 μM) for 3 h before being harvested and lysed in SDS lysis buffer. The cell lysates were boiled for 10 min, diluted 10 times with IP lysis buffer (10 mM Hepes at pH7.4, 142.5 mM KCl, 5 mM $MgCl_2$, 1 mM EGTA and 1% NP-40) and immunoprecipitated with anti-FLAG agarose-conjugated beads. The precipitates were extensively washed and analyzed by western blotting using an HRP-conjugated anti-HA antibody (Roche, Basel, Switzerland) or anti-ubiquitin, Lys48-Specific (Millipore, 05-1307).

SNIPER-mediated interaction of TACC3 and APC/C^{CDH1}. Cells were co-transfected for 40 h with the expression vectors of Flag-TACC3 and Myc-CDH1 and treated for 3 h with MG132 in the presence or absence of SNIPER (TACC3)-1. Cells were lysed with IP lysis buffer (10 mM Hepes at pH 7.4, 142.5 mM KCl, 5 mM $MgCl_2$, 1 mM EGTA and 0.1% Triton X-100) containing a protease inhibitor cocktail, rotated for 15 min at 4 °C and centrifuged at 15 000 r.p.m. for 10 min at 4 °C to obtain the supernatants. The lysates, which had been precleared with naked protein G-sepharose, were immunoprecipitated with anti-FLAG agarose-conjugated beads for 2 h at 4 °C. The precipitates were washed with IP lysis buffer four times and eluted by mild vortexing with IP lysis buffer containing the compounds for 15 min at room temperature. After centrifugation at 15 000 r.p.m. for 1 min, the eluted fractions (the supernatants) were obtained and analyzed by western blotting.

Thermal shift assay. Thermal shift assay was performed as previously described.[32] Cells were harvested and washed with PBS. The cells were suspended in kinase buffer (25 mM Tris(hydroxymethyl)-aminomethane hydrochloride (Tris-HCl, pH 7.5), 5 mM beta-glycerophosphate, 2 mM dithiothreitol, 0.1 mM sodium vanadium oxide, 10 mM magnesium chloride) (Cell Signaling Technology) supplemented with protease inhibitor cocktail. The cell suspensions were freeze-thawed three times using liquid nitrogen and centrifuged at 15 000 r.p.m. for 10 min at 4 °C to obtain the supernatants (lysate). The cell lysates were divided into four aliquots, with each aliquot being treated with each compound or DMSO (control). After 10–30 min incubation at room temperature, the respective lysates were divided into smaller (50 μl) aliquots and heated individually at graded temperatures for 3 min (PCR thermal cycler, Applied Biosystems/Life Technologies, Carlsbad, CA, USA) followed by cooling for 3 min at room temperature. The heated lysates were centrifuged at 15 000 r.p.m. for 10 min at 4 °C in order to separate the soluble fractions from precipitates. The supernatants were transferred to new microtubes and analyzed by SDS-PAGE followed by western blotting.

Cell viability assay. Cell viability was determined using water-soluble tetrazolium WST-8 (4-[3-(2-methoxy-4-nitrophenyl)-2-(4-nitrophenyl)-2H-5-tetrazolio]-1,3-benzene disulfonate) for the spectrophotometric assay according to the manufacturer's instructions (Dojindo, Tokyo, Japan). Cells were seeded at a concentration of 5×10^3 cells per well in a 96-well culture plate. After 24 h, cells were treated with the indicated compounds for 48 h. The WST-8 reagent was added, and the cells were incubated for 0.5 h at 37 °C in a humidified atmosphere of 5% CO_2. The absorbance at 450 nm of the medium was measured using an EnVision Multilabel Plate Reader (PerkinElmer, Waltham, MA, USA).

Measurement of apoptosis by flow cytometer. Apoptosis was analyzed with an Annexin V-FITC Apoptosis Detection Kit (BioVision, Milpitas, CA, USA). After treatment, cells were gently trypsinized and washed with serum-containing medium. Cells were collected by centrifugation, and additionally washed with PBS, and resuspended in Binding Buffer. The cells were stained with annexin V-FITC and PI at room temperature for 5 min in the dark, according to the manufacturer's instructions, and analyzed on a FACScan flow cytometer (Becton Dickinson, Braintree, MA, USA).

Cell cycle analysis. After treatment, cells were gently trypsinized and washed with serum-containing medium. Cells were collected by centrifugation, and additionally washed with PBS, and fixed in 70% ice-cold ethanol for 1 h on ice. The cells were then washed, treated with 1 mg/ml RNase A for 1 h at 37 °C and stained in PI solution (50 μg/ml in 0.1% sodium citrate, 0.1% NP-40). The stained cells were analyzed on a FACScan flow cytometer (Becton Dickinson).

Conflict of Interest

K Nagai and N Cho are employees of Takeda Pharmaceutical Co., Ltd. (Osaka, Japan). M Naito received a research fund from Takeda Pharmaceutical Co., Ltd. The other authors declare no conflict of interest.

Acknowledgements. We thank Dr. N Miyamoto, Dr. M Ito and Dr. Y Morita for helpful discussions, and Dr. R Yao for information on TACC3. This study was supported by Grants-in Aid for Scientific Research from the Japan Society for the Promotion of Science (to MN and NO) and Research Fund from the Japan Health Sciences Foundation (to MN). Pacific Edit reviewed the manuscript prior to submission.

1. Sudakin V, Yen TJ. Targeting mitosis for anti-cancer therapy. *BioDrugs* 2007; **21**: 225–233.
2. Lens SM, Voest EE, Medema RH. Shared and separate functions of polo-like kinases and aurora kinases in cancer. *Nat Rev Cancer* 2010; **10**: 825–841.
3. Jackson JR, Patrick DR, Dar MM, Huang PS. Targeted anti-mitotic therapies: can we improve on tubulin agents? *Nat Rev Cancer* 2007; **7**: 107–117.
4. Hood FE, Royle SJ. Pulling it together: the mitotic function of TACC3. *Bioarchitecture* 2011; **1**: 105–109.
5. Gergely F, Karlsson C, Still I, Cowell J, Kilmartin J, Raff JW. The TACC domain identifies a family of centrosomal proteins that can interact with microtubules. *Proc Natl Acad Sci USA* 2000; **97**: 14352–14357.
6. LeRoy PJ, Hunter JJ, Hoar KM, Burke KE, Shinde V, Ruan J *et al.* Localization of human TACC3 to mitotic spindles is mediated by phosphorylation on Ser558 by Aurora A: a novel pharmacodynamic method for measuring Aurora A activity. *Cancer Res* 2007; **67**: 5362–5370.
7. Lin CH, Hu CK, Shih HM. Clathrin heavy chain mediates TACC3 targeting to mitotic spindles to ensure spindle stability. *J Cell Biol* 2010; **189**: 1097–1105.
8. Booth DG, Hood FE, Prior IA, Royle SJ. A TACC3/ch-TOG/clathrin complex stabilises kinetochore fibres by inter-microtubule bridging. *EMBO J* 2011; **30**: 906–919.
9. Fu W, Tao W, Zheng P, Fu J, Bian M, Jiang Q *et al.* Clathrin recruits phosphorylated TACC3 to spindle poles for bipolar spindle assembly and chromosome alignment. *J Cell Sci* 2010; **123**(Pt 21): 3645–3651.
10. Lioutas A, Vernos I. Aurora A kinase and its substrate TACC3 are required for central spindle assembly. *EMBO Rep* 2013; **14**: 829–836.
11. Hood FE, Williams SJ, Burgess SG, Richards MW, Roth D, Straube A *et al.* Coordination of adjacent domains mediates TACC3-ch-TOG-clathrin assembly and mitotic spindle binding. *J Cell Biol* 2013; **202**: 463–478.
12. Ma XJ, Salunga R, Tuggle JT, Gaudet J, Enright E, McQuary P *et al.* Gene expression profiles of human breast cancer progression. *Proc Natl Acad Sci USA* 2003; **100**: 5974–5979.
13. Jacquemier J, Ginestier C, Rougemont J, Bardou VJ, Charafe-Jauffret E, Geneix J *et al.* Protein expression profiling identifies subclasses of breast cancer and predicts prognosis. *Cancer Res* 2005; **65**: 767–779.

14. Lauffart B, Vaughan MM, Eddy R, Chervinsky D, DiCioccio RA, Black JD *et al.* Aberrations of TACC1 and TACC3 are associated with ovarian cancer. *BMC Womens Health* 2005; **5**: 8.
15. Kimura M, Yoshioka T, Saio M, Banno Y, Nagaoka H, Okano Y. Mitotic catastrophe and cell death induced by depletion of centrosomal proteins. *Cell Death Dis* 2013; **4**: e603.
16. Piekorz RP, Hoffmeyer A, Duntsch CD, McKay C, Nakajima H, Sexl V *et al.* The centrosomal protein TACC3 is essential for hematopoietic stem cell function and genetically interfaces with p53-regulated apoptosis. *EMBO J* 2002; **21**: 653–664.
17. Schmidt S, Schneider L, Essmann F, Cirstea IC, Kuck F, Kletke A *et al.* The centrosomal protein TACC3 controls paclitaxel sensitivity by modulating a premature senescence program. *Oncogene* 2010; **29**: 6184–6192.
18. Schneider L, Essmann F, Kletke A, Rio P, Hanenberg H, Schulze-Osthoff K *et al.* TACC3 depletion sensitizes to paclitaxel-induced cell death and overrides p21WAF-mediated cell cycle arrest. *Oncogene* 2008; **27**: 116–125.
19. Schneider L, Essmann F, Kletke A, Rio P, Hanenberg H, Wetzel W *et al.* The transforming acidic coiled coil 3 protein is essential for spindle-dependent chromosome alignment and mitotic survival. *J Biol Chem* 2007; **282**: 29273–29283.
20. Yao R, Natsume Y, Noda T. TACC3 is required for the proper mitosis of sclerotome mesenchymal cells during formation of the axial skeleton. *Cancer Sci* 2007; **98**: 555–562.
21. Yao R, Natsume Y, Saiki Y, Shioya H, Takeuchi K, Yamori T *et al.* Disruption of Tacc3 function leads to in vivo tumor regression. *Oncogene* 2012; **31**: 135–148.
22. Okuhira K, Ohoka N, Sai K, Nishimaki-Mogami T, Itoh Y, Ishikawa M *et al.* Specific degradation of CRABP-II via cIAP1-mediated ubiquitylation induced by hybrid molecules that crosslink cIAP1 and the target protein. *FEBS Lett* 2011; **585**: 1147–1152.
23. Itoh Y, Ishikawa M, Naito M, Hashimoto Y. Protein knockdown using methyl bestatin-ligand hybrid molecules: design and synthesis of inducers of ubiquitination-mediated degradation of cellular retinoic acid-binding proteins. *J Am Chem Soc* 2010; **132**: 5820–5826.
24. Itoh Y, Kitaguchi R, Ishikawa M, Naito M, Hashimoto Y. Design, synthesis and biological evaluation of nuclear receptor-degradation inducers. *Bioorg Med Chem* 2011; **19**: 6768–6778.
25. Itoh Y, Ishikawa M, Kitaguchi R, Sato S, Naito M, Hashimoto Y. Development of target protein-selective degradation inducer for protein knockdown. *Bioorg Med Chem* 2011; **19**: 3229–3241.
26. Itoh Y, Ishikawa M, Kitaguchi R, Okuhira K, Naito M, Hashimoto Y. Double protein knockdown of cIAP1 and CRABP-II using a hybrid molecule consisting of ATRA and IAPs antagonist. *Bioorg Med Chem Lett* 2012; **22**: 4453–4457.
27. Demizu Y, Okuhira K, Motoi H, Ohno A, Shoda T, Fukuhara K *et al.* Design and synthesis of estrogen receptor degradation inducer based on a protein knockdown strategy. *Bioorg Med Chem Lett* 2012; **22**: 1793–1796.
28. Okuhira K, Demizu Y, Hattori T, Ohoka N, Shibata N, Nishimaki-Mogami T *et al.* Development of hybrid small molecules that induce degradation of estrogen receptor-alpha and necrotic cell death in breast cancer cells. *Cancer Sci* 2013; **24**: 87–89.
29. Sekine K, Takubo K, Kikuchi R, Nishimoto M, Kitagawa M, Abe F *et al.* Small molecules destabilize cIAP1 by activating auto-ubiquitylation. *J Biol Chem* 2008; **283**: 8961–8968.
30. Jeng JC, Lin YM, Lin CH, Shih HM. Cdh1 controls the stability of TACC3. *Cell Cycle* 2009; **8**: 3529–3536.
31. Peters JM. The anaphase promoting complex/cyclosome: a machine designed to destroy. *Nat Rev Mol Cell Biol* 2006; **7**: 644–656.
32. Martinez Molina D, Jafari R, Ignatushchenko M, Seki T, Larsson EA, Dan C *et al.* Monitoring drug target engagement in cells and tissues using the cellular thermal shift assay. *Science* 2013; **341**: 84–87.
33. Malumbres M, Barbacid M. Cell cycle, CDKs and cancer: a changing paradigm. *Nat Rev Cancer* 2009; **9**(3): 153–166.
34. Ha GH, Kim JL, Breuer EK. Transforming acidic coiled-coil proteins (TACCs) in human cancer. *Cancer Lett* 2013; **336**: 24–33.
35. Cappell KM, Sinnott R, Taus P, Maxfield K, Scarbrough M, Whitehurst AW. Multiple cancer testis antigens function to support tumor cell mitotic fidelity. *Mol Cell Biol* 2012; **32**: 4131–4140.
36. Guo G, Sun X, Chen C, Wu S, Huang P, Li Z *et al.* Whole-genome and whole-exome sequencing of bladder cancer identifies frequent alterations in genes involved in sister chromatid cohesion and segregation. *Nat Genet* 2013; **45**: 1459–1463.
37. Kiemeney LA, Sulem P, Besenbacher S, Vermeulen SH, Sigurdsson A, Thorleifsson G *et al.* A sequence variant at 4p16.3 confers susceptibility to urinary bladder cancer. *Nat Genet* 2010; **42**: 415–419.
38. Parker BC, Annala MJ, Cogdell DE, Granberg KJ, Sun Y, Ji P *et al.* The tumorigenic FGFR3-TACC3 gene fusion escapes miR-99a regulation in glioblastoma. *J Clin Invest* 2013; **123**: 855–865.
39. Shinmura K, Kato H, Matsuura S, Inoue Y, Igarashi H, Nagura K *et al.* A novel somatic FGFR3 mutation in primary lung cancer. *Oncol Rep* 2014; **31**: 1219–1224.
40. Singh D, Chan JM, Zoppoli P, Niola F, Sullivan R, Castano A *et al.* Transforming fusions of FGFR and TACC genes in human glioblastoma. *Science* 2012; **337**: 1231–1235.
41. Williams SV, Hurst CD, Knowles MA. Oncogenic FGFR3 gene fusions in bladder cancer. *Hum Mol Genet* 2013; **22**: 795–803.
42. Yao R, Kondoh Y, Natsume Y, Yamanaka H, Inoue M, Toki H *et al.* A small compound targeting TACC3 revealed its different spatiotemporal contributions for spindle assembly in cancer cells. *Oncogene* 2013; **33**: 4242–4252.
43. Wurdak H, Zhu S, Min KH, Aimone L, Lairson LL, Watson J *et al.* A small molecule accelerates neuronal differentiation in the adult rat. *Proc Natl Acad Sci USA* 2010; **107**: 16542–16547.
44. Ohoka N, Sakai S, Onozaki K, Nakanishi M, Hayashi H. Anaphase-promoting complex/cyclosome-cdh1 mediates the ubiquitination and degradation of TRB3. *Biochem Biophys Res Commun* 2010; **392**: 289–294.

Supplementary Information accompanies this paper on Cell Death and Disease website (http://www.nature.com/cddis)

Bioconjugate Chemistry

Communication

pubs.acs.org/bc

Development of Cell-Penetrating R7 Fragment-Conjugated Helical Peptides as Inhibitors of Estrogen Receptor-Mediated Transcription

Takaya Nagakubo,[†,‡] Yosuke Demizu,[*,†] Yasunari Kanda,[†] Takashi Misawa,[†] Takuji Shoda,[†] Keiichiro Okuhira,[†] Yuko Sekino,[†] Mikihiko Naito,[†] and Masaaki Kurihara[*,†,‡]

[†]National Institute of Health Sciences, Tokyo 158-8501, Japan

[‡]Graduate School of Bioscience and Biotechnology, Tokyo Institute of Technology, Yokohama 226-8501, Japan

Supporting Information

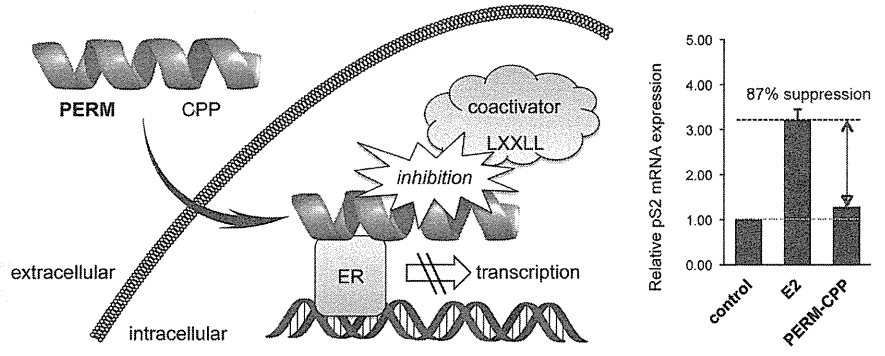

ABSTRACT: The heptaarginine (R7)-conjugated peptide **5** was designed and synthesized as an inhibitor of ER-coactivator interactions and ER-mediated transcription at the cellular level. The R7-conjugated peptide **5** was able to enter ER-positive T47D cells efficiently, and treatment with 3 μM of **5** downregulated the mRNA expression of pS2 (an ER-mediated gene) by 87%.

INTRODUCTION

Breast cancer is the most common cancer in women, and its incidence is increasing from year to year. The estrogen receptor (ER), which is a ligand-inducible transcription factor and a member of the nuclear receptor superfamily, is often overexpressed in the tissues of breast cancer patients and promotes the estrogen-dependent proliferation of cancer cells.[1−3] Several ERα antagonistic drugs, such as tamoxifen and nonsteroidal selective ER modulators, have been developed as treatments for breast cancer.[4−8] Among those antagonists, tamoxifen acts via the competitive inhibition of 17β-estradiol (E2) and is the most widely used drug for treating breast cancer.[9,10] However, tamoxifen has agonistic effects on ERα in uterine cancer cells and increases the risk of endometrial cancer.[11,12] In addition, it activates the protein kinase B (Akt) signaling pathway by binding to a particular ER variant, resulting in the inhibition of apoptosis in cancer cells.[13,14] Therefore, novel drug candidates with different mechanisms of action have long been desired. ER-mediated gene activation is induced by the binding of E2 to the ER ligand-binding domain and the subsequent binding of the consensus LXXLL helical motif[15] (L: leucine, X: any amino acid residue) of the coactivator with the ER surface.[16,17] Helical peptides containing the above-mentioned consensus sequence have been demonstrated to inhibit ER-coactivator interactions, and they are also considered to be drug candidates for reducing ER-mediated transactivation. Various helical peptides have been reported as inhibitors of ER-coactivator interactions.[18−22] The peptidomimetic estrogen receptor modulators (PERMs), specifically, PERM-1 and PERM-3 [with two mutation: Lys(1) → Arg(1) and Leu(7) → Npg(7)] reported by Burris et al. exhibited particularly potent inhibitory activity against ER-coactivator interactions.[19,20] However, only a few peptide-based ER-transcription inhibitors that exhibit potent activity at the cellular level have been reported[23,24] because of the low cell permeability of such peptides. Thus, we assumed that the conjugation of PERM with cell-penetrating peptides such as oligoarginines and their derivatives[25,26] might solve the problems surrounding the development of novel peptide-based transcriptional inhibitors (Figure 1). In this communication, we describe the synthesis of heptaarginine (R7)-conjugated PERM as inhibitors of ER-signaling at the cellular level (Table 1). Specifically, we synthesized R7-conjugated helical peptides and evaluated their cellular uptake, ability to inhibit transcription in ER-positive T47D cells, ability to inhibit ER-coactivator interactions, and their preferred secondary structures (by assessing their CD spectra).

RESULTS AND DISCUSSION

Synthesis of Peptides. The N-terminal-free peptides **1**−**7** and their N-terminal fluorescein (FAM) labeled peptides were

Received: October 17, 2014
Revised: November 5, 2014
Published: November 6, 2014

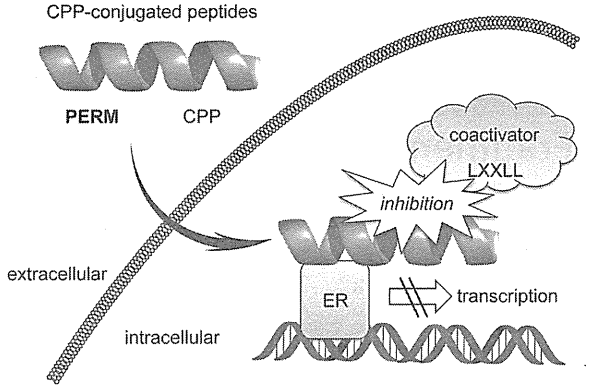

Figure 1. Illustration of the mechanism by which the CPP-conjugated peptides inhibited ER-coactivator interactions at the cellular level.

synthesized using microwave-assisted Fmoc-based solid phase methods, respectively. All of the peptides were purified by reversed-phase high performance liquid chromatography and were characterized using electrospray ionization time-of-flight mass spectrometry (Supporting Information).

Biological Evaluations. First of all, we evaluated the cellular uptake of fluorescein-labeled peptides (green; 1 μM) into ER-positive T47D cells (incubated for 3 h) using confocal laser scanning microscopy (CLSM, Supporting Information) as shown in Figure 2. The R7-unconjugated peptide **FAM-2** (an N-terminal fluorescein-labeled version of peptide **2**) was completely unable to enter the ER-positive T47D cells, whereas the R7-conjugated peptide **FAM-5** passed through the cell membrane efficiently and was distributed in the cytoplasm and nucleus. This difference in the cell-penetrating abilities of the molecules was solely due to the presence/absence of R7 conjugation. The R7-conjugated peptide **FAM-4** also exhibited cell permeability (Supporting Information).

Then, we evaluated the ability of the R7-conjugated peptides to inhibit ER-mediated transcription. Transcriptional analysis of an ER target gene (pS2) was carried out using T47D cells that had been incubated with one of the peptides (3 μM) in the absence or presence of 10 nM E2 for 24 h. The mRNA expression of pS2, which is the one gene whose expression is upregulated by E2, was analyzed using the quantitative polymerase chain reaction (Supporting Information). The relative pS2 mRNA expression levels of the cells treated with each peptide are summarized in Figure 3. The R7-unconjugated (nonmembrane-penetrating) peptides **1**–**3** and the heptaarginine (YR7)[27] peptide did not inhibit transcription. On the other hand, the mRNA expression of pS2 was significantly decreased (by 87%) by the addition of 3 μM of the R7-conjugated peptide **5**. Treatment with 3 μM of the R7-conjugated peptide **4** did not suppress the mRNA expression of pS2 at all, but treatment with 10 μM of **4** decreased it by 95% (Supporting Information). Conversely, treatment with the R7-conjugated peptide **6** at concentrations ranging from 3 μM to 10 μM did not induce any significant reduction in ER-mediated transcriptional activity. These results demonstrated that the R7-conjugated peptides **4** and **5** were able to exhibit antagonistic effects on ER-mediated transcription at the cellular level, and **5** displayed particularly potent inhibitory activity.

The inhibitory activity of peptides **4** and **5** against ER–coactivator interactions were evaluated using EnBio receptor cofactor assay systems (RCAS) for ERα (Fujikura Kasei Co., Ltd.) according to the manufacturer's instructions (Figure 4). The R7-unconjugated peptides **1** and **2** demonstrated strong activity against ERα–coactivator interactions. While the activities of the corresponding R7-conjugated peptides **4** and **5** were reduced, peptide **5** still demonstrated strong activity (IC_{50}: 94 nM). These results indicated that peptides **4** and **5** suppress ER-mediated transcription by inhibiting ERα–coactivator interactions. The R7-conjugated peptide **5** exhibited stronger inhibitory activity against ERα–coactivator interactions than **4**, and therefore, **5** was able to suppress ER-mediated transcription more efficiently than **4**, even at the cellular level.

The dominant conformations of peptides **1**–**6** were analyzed by assessing their CD spectra in 20% aqueous 2,2,2-trifluoroethanol (TFE) solution (Figure 5). The CD spectra of peptides **1** and **2**, and those of their R7-conjugated peptides **4** and **5**, displayed negative maxima at around 208 and 222 nm, indicating that all of the peptides formed stable right-handed α-helical structures. These findings suggested that the R7 fragment did not disrupt helix formation. On the other hand, the SRC-1 peptide **3** and its R7-conjugated form **6** were found to be composed of random coil structures rather than α-helices. These results indicated that peptides require stabilized helical structures in order to possess significant inhibitory activity against ER-coactivator interactions.

CONCLUSION

In conclusion, we developed heptaarginine (R7)-conjugated PERM as molecules that could be used to suppress ER-mediated transcription at the cellular level. The R7-conjugated peptides were able to enter ER-positive T47D cells efficiently, and one of them, peptide **5**, downregulated the mRNA expression of pS2 by 87% at a dose of 3 μM. Furthermore, **5** displayed strong inhibitory activity (IC_{50}: 94 nM) against ER–coactivator interactions. Although the inhibitory activity of the R7-conjugated peptide **5** against ER–coactivator interactions was slightly decreased compared with that of the R7-unconjugated peptide **2** (IC_{50}: 13 nM), **5** still exhibited potent activity. The dominant conformations of the peptides were analyzed based on

Table 1. Sequences of Peptides 1–7

peptide	sequence
PERM-1 (**1**)	H-Lys-*cyclo*(D-Cys-Ile-Leu-Cys)-Arg-Leu-Leu-Gln-NH_2
PERM-3 (**2**)	H-Arg-*cyclo*(D-Cys-Ile-Leu-Cys)-Arg-Npg[a]-Leu-Gln-NH_2
SRC-1[b] (**3**)	H-His-Lys-Ile-Leu-His-Arg-Leu-Leu-Gln-NH_2
PERM-1-R7 (**4**)	H-Lys-*cyclo*(D-Cys-Ile-Leu-Cys)-Arg-Leu-Leu-Gln-$(Gly)_3$-$(Arg)_7$-NH_2
PERM-3-R7 (**5**)	H-Arg-*cyclo*(D-Cys-Ile-Leu-Cys)-Arg-Npg-Leu-Gln-$(Gly)_3$-$(Arg)_7$-NH_2
SRC-1-R7 (**6**)	H-His-Lys-Ile-Leu-His-Arg-Leu-Leu-Gln-$(Gly)_3$-$(Arg)_7$-NH_2
YR7 (**7**)	H-Tyr-$(Arg)_7$-NH_2

[a]Npg: neopentylglycine. [b]The LXXLL motif of the coactivator.

dx.doi.org/10.1021/bc500480e | *Bioconjugate Chem.* 2014, 25, 1921–1924